

In situ deployment of engineered extracellular vesicles into the tumor niche via myeloid-derived suppressor cells

*Silvia Duarte-Sanmiguel¹Ψ, Ana Panic¹Ψ, Daniel Dodd^{1,2}Ψ, Ana Salazar-Puerta¹, Jordan T. Moore¹, William R. Lawrence², Kylie Nairon¹, Carlie Francis¹, Natalie Zachariah¹, Billy McCoy¹, Rithvik Turaga¹, Aleksander Skardal¹, William E. Carson³, Natalia Higueta-Castro^{1,3,4}, Daniel Gallego-Perez^{1,3}**

¹ The Ohio State University, Department of Biomedical Engineering, Columbus, OH 43210

² The Ohio State University, Biomedical Sciences Graduate Program, Columbus, OH 43210

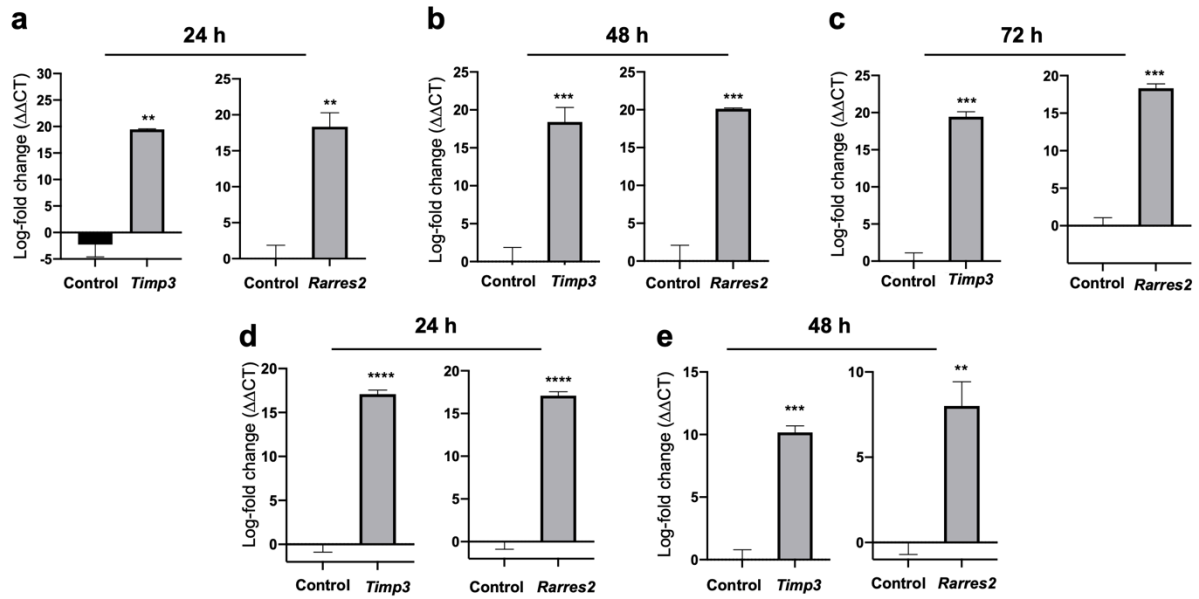
³The Ohio State University, Department of Surgery, Columbus, OH 43210

⁴The Ohio State University, Biophysics Program, OH 43210

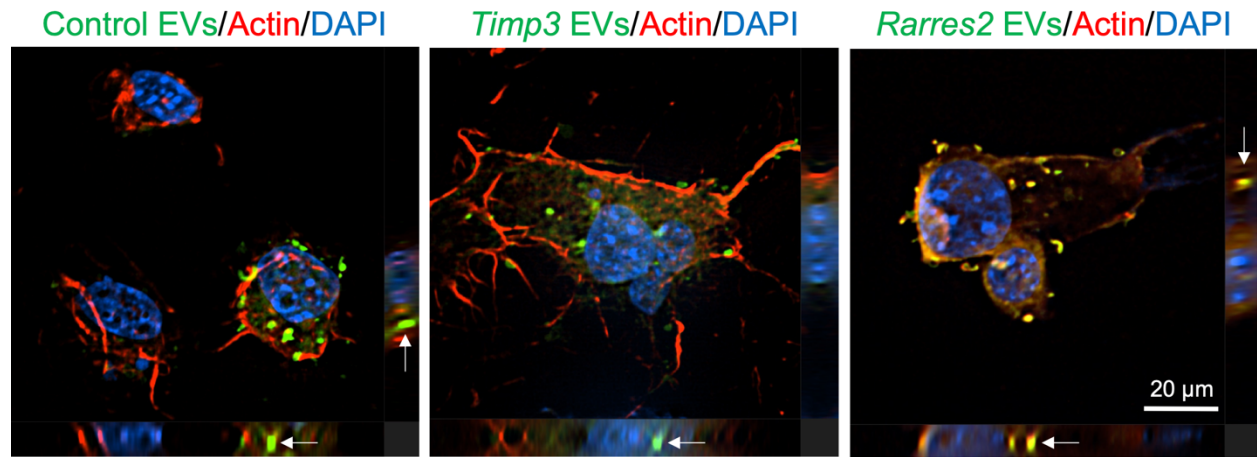
ΨEqual contribution

*To whom correspondence should be addressed: gallegoperez.1@osu.edu

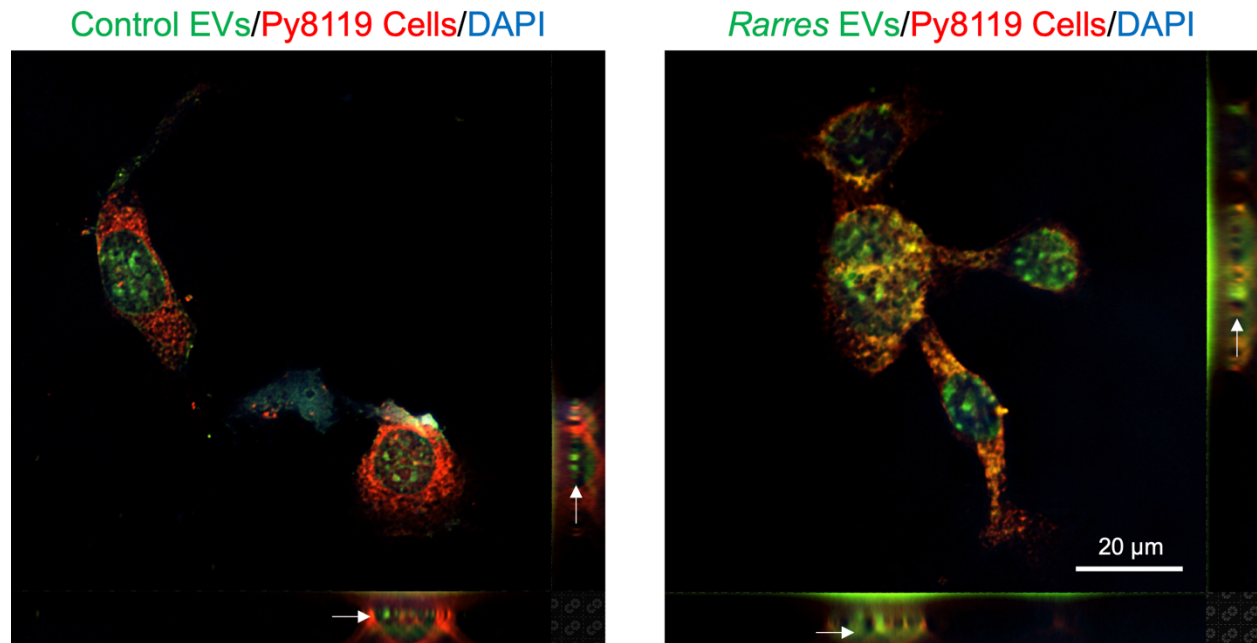
higuitacastro.1@osu.edu



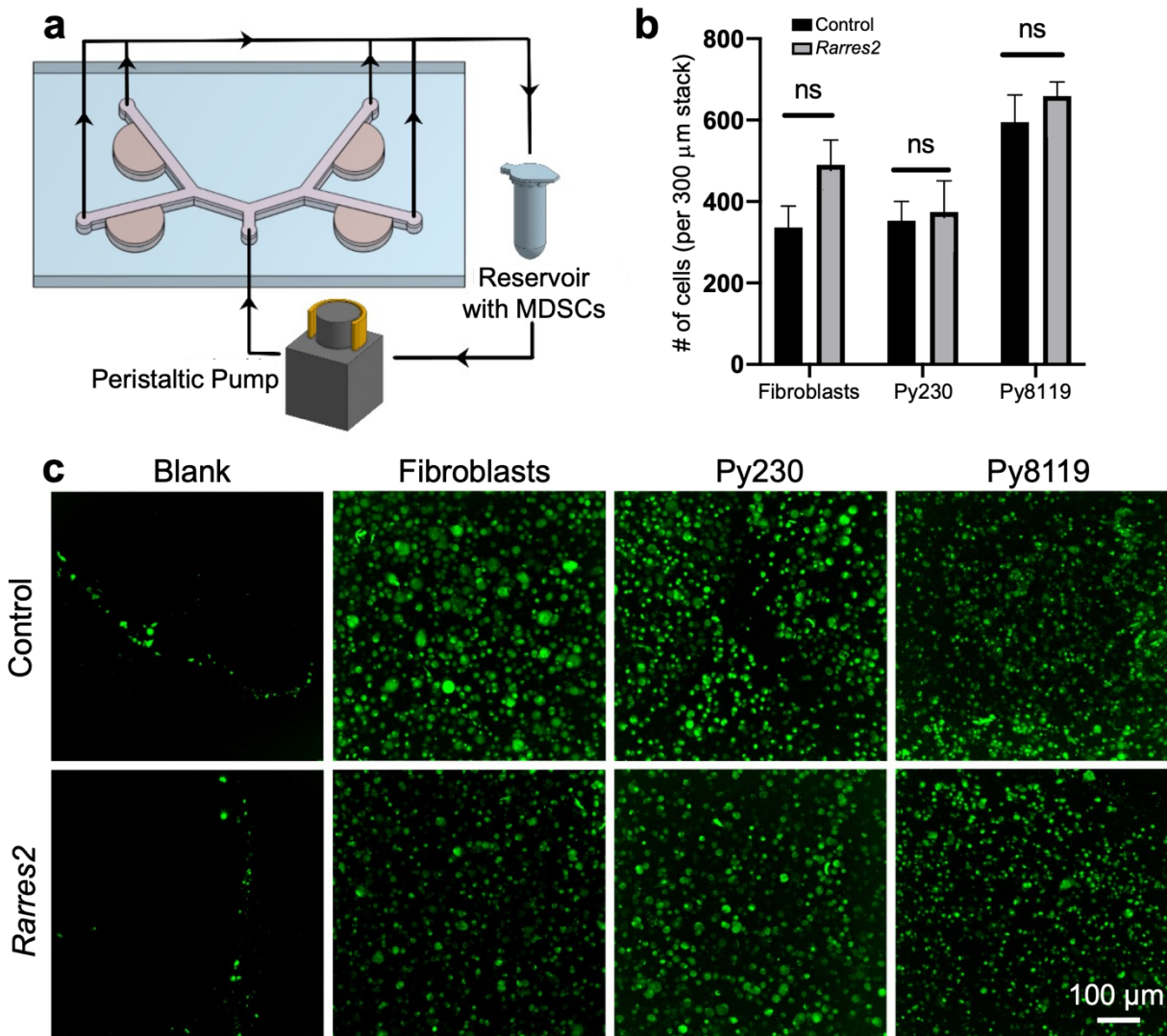
Supplementary Fig. 1. Non-viral co-transfection of *Timp3* and *Rarress2* results in effective co-loading of EVs. qRT-PCR analysis of the co-transfected MDSC cultures at **(b)** 24, **(c)** 48, and **(d)** 72 hours post-electroporation reveals strong *Timp3* and *Rarress2* co-overexpression. Analysis of the EVs isolated from the supernatant at **(f)** 24 and **(g)** 48 hours post-electroporation indicates successful co-loading of the EVs with *Timp3* and *Rarress2*. ** $p < 0.05$ (n= 3), *** $p < 0.001$ (n= 3), **** $p < 0.0001$ (n= 3).



Supplementary Fig. 2. Z-stack images of breast cancer cells (red) exposed to MDSC-derived EVs (green). Orthogonal projections of the z-stack (right and bottom) in each micrograph show EVs successfully internalized by breast cancer cells (white arrows).



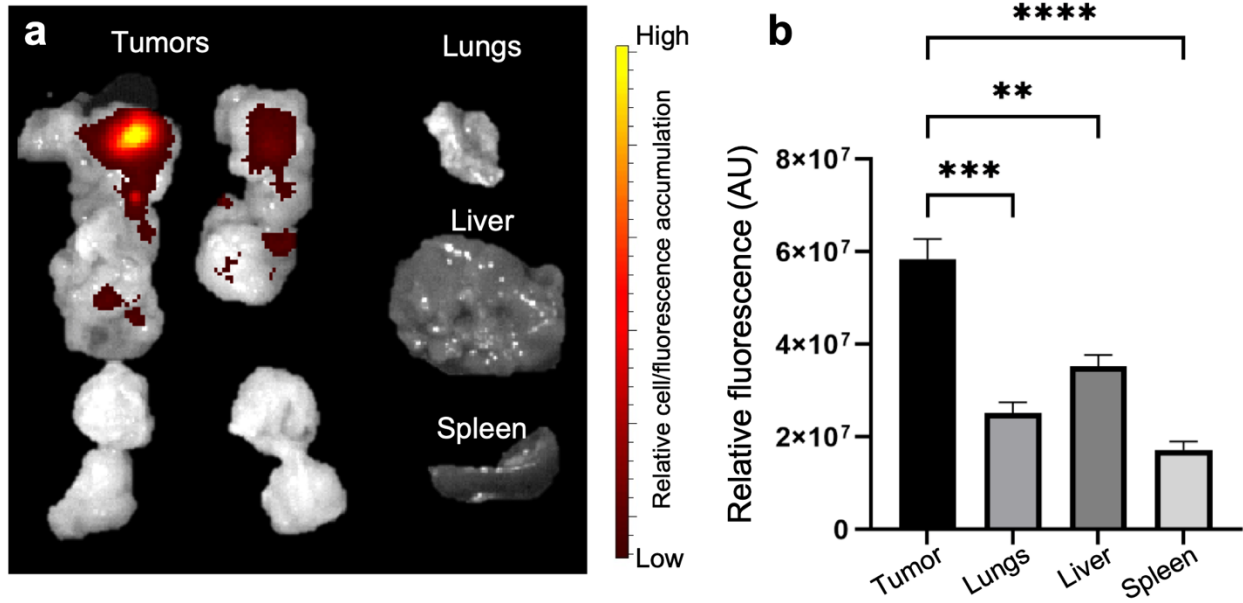
Supplementary Fig. 3. Z-stack images of breast cancer cells (red) co-cultured with prelabeled MDSCs in a transwell insert. MDSCs were plated in the apical portion of the insert, while breast cancer cells were plated in the basal portion. Insert pore size was ~400 nm to enable translocation of MDSC-derived EVs (green). Orthogonal projections of the z-stack (right and bottom) in each micrograph show that EVs derived from MDSCs (*in situ*) were successfully internalized by breast cancer cells (white arrows).



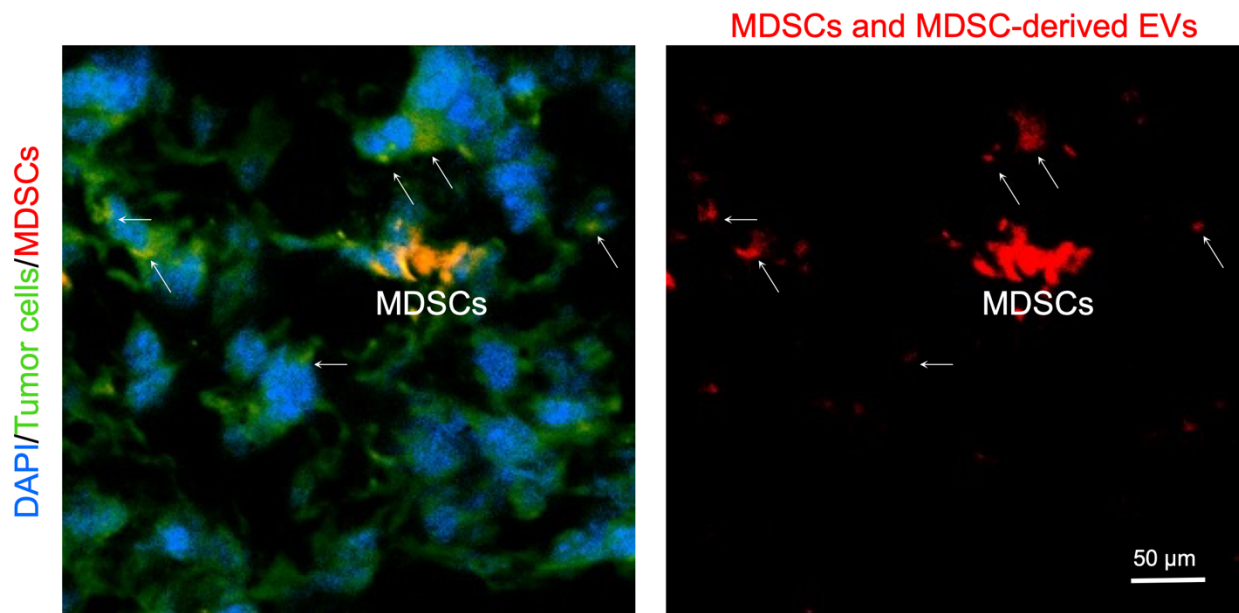
Supplementary Fig. 4. *Ex vivo* infiltration assays with cancerous and non-cancerous cell organoids revealed that transfected MDSCs retain their ability to invade target tissues. (a) Microfluidic devices were designed to contain 4 semi-cylindrical chambers (5 mm diameter, 1 mm height) connected by branching channels to a single inlet and 4 discrete outlets. Devices were fabricated via traditional replica molding of polydimethylsiloxane (PDMS) using a laser cut polymethylmethacrylate (PMMA) master mold. The completed PDMS layer and a clean glass slide were then N₂ plasma-activated for 60 seconds and irreversibly bonded to form the sealed device.

Fluidic connections were completed using PTFE tubing (Cole-Parmer) and 2-stop PVC 0.51 mm inner diameter pump tubing (Elemental Scientific), with a media reservoir/bubble trap to provide an adequate nutrient flow. A single line of PTFE tubing was used to connect the reservoir to the inlet port of the device, with the pump incorporated between to induce pressure-driven flow. Four separate tubing lines connected the discrete outlet ports back to the media reservoir, thus completing the fluidic circuit. Primary mouse embryonic fibroblasts (PMEF), and PY230, or PY8119 breast cancer cells were suspended in hydrogel precursor solutions consisting of 3:1 methacrylated collagen I and thiolated hyaluronic acid^{1,2}. Briefly, thiolated hyaluronic acid (Advanced Biomatrix) was reconstituted at 1 mg/mL in sterile, degassed water containing 0.01% w/v photoinitiator (2-Hydroxy-4'-(2-hydroxyethoxy)-2-methylpropiophenone, Sigma). Methacrylated collagen I (Advanced Biomatrix) was dissolved in sterile-filtered 20 mM acetic acid to a final concentration of 6 mg/mL at 4°C. Directly prior to use, collagen aliquots were neutralized with a sodium hydroxide neutralization solution (Advanced Biomatrix). The collagen and hyaluronic acid solutions were then combined at a 3:1 ratio and used to resuspend cells at 5000 cells/ μ L. Cell-laden hydrogel precursors were injected into their respective microfluidic chambers and crosslinked in situ with a 365 nm UV light for 2 seconds. An acellular hydrogel was similarly implanted into the device as a negative control. To allow MDSC circulation throughout the system, sham- or *Rarres2*-transfected MDSCs (green) were perfused through the device using a microperistaltic pump (Elemental Scientific) at 10 μ L/minute for 24 hours. At the end of this period, the embedded hydrogel constructs with infiltrative MDSCs were retrieved from the devices and imaged using a Nikon A1R Live Cell Imaging Confocal Microscope (Nikon). Z-stacks of 300 μ m were taken for each hydrogel construct, from which 2D maximum projection images were formed, allowing quantification of all green (MDSC) tagged cells. The NIS-Elements image

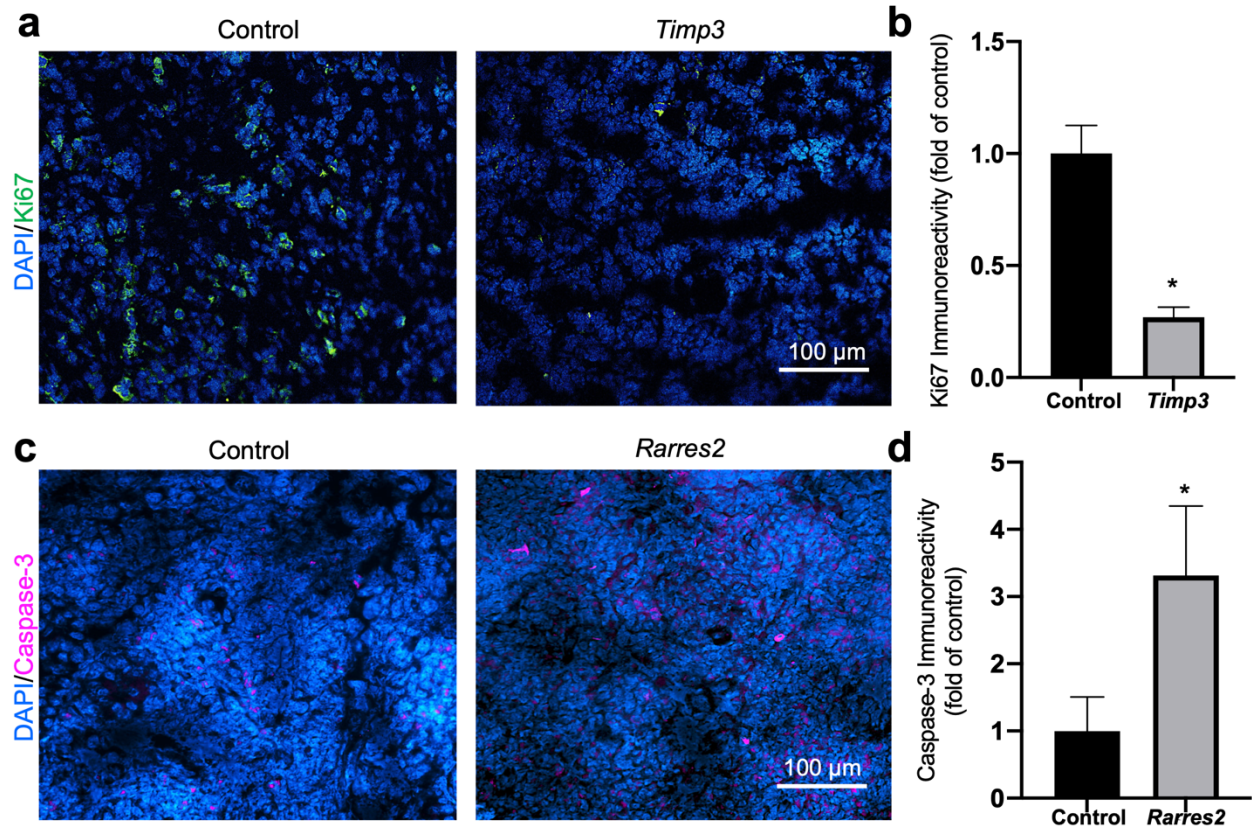
analysis program's object count feature was used for objective cell quantification in MDSC infiltration studies. **(b, c)** Quantification of MDSC infiltration revealed similar infiltration/homing levels for MDCs transfected with sham vs. *Rarres2* plasmids, thus suggesting that therapeutic transgene expression does not have an impact on the ability of these cells to invade target tissues.



Supplementary Fig. 5. (a) *Rarres2*-transfected MDSCs preferentially accumulate in the tumor in a mouse model of breast cancer. **(b)** Little to no accumulation is seen in clearance organs such as the liver or spleen. ** $p < 0.01$ (n= 4), *** $p < 0.001$ (n= 4), **** $p < 0.0001$ (n= 4).



Supplementary Fig. 6. MDSC-derived EVs are deployed and internalized by other cells within the tumor niche. Orthotropic breast tumor xenografts were pre-labeled green, and MDSCs were pre-labeled red with a membrane dye that enables tracing of EV release. MDSCs were deployed via tail vein injection, and the tumors were collected and processed for imaging 24 hours post-injection. Imaging of tumor tissue sections shows MDSCs (red) and MDSC-derived EVs being internalized by the xenografted tumor cells (arrows).



Supplementary Fig. 7. MDSC-driven overexpression of *Timp3* and *Rarress2* in the tumor niche modulates anti-tumoral responses. (a, b) MDSC-driven deployment of *Timp3*-loaded EVs correlated with a decrease in Ki67 immunoreactivity in the tumor niche, indicative of reduced cell proliferation. **(c, d)** MDSC-driven deployment of *Rarress2*--loaded EVs correlated with an increase in cleaved caspase-2 immunoreactivity, indicative of enhanced pro-apoptotic activity.

* $p < 0.05$ (n= 7-9).

REFERENCES

- 1 Maloney, E. *et al.* Immersion bioprinting of tumor organoids in multi-well plates for increasing chemotherapy screening throughput. *Micromachines* **11**, 208 (2020).
- 2 Mazzocchi, A., Devarasetty, M., Huntwork, R., Soker, S. & Skardal, A. Optimization of collagen type I-hyaluronan hybrid bioink for 3D bioprinted liver microenvironments. *Biofabrication* **11**, 015003 (2018).